

Experimental study on hollow steel-reinforced concrete-filled GFRP tubular members under axial compression

B.L. Chen^a and L.G. Wang^{*}

College of Resources and Civil Engineering, Northeastern University, Shenyang 110819, P.R. China

(Received June 2, 2018, Revised April 7, 2019, Accepted May 31, 2019)

Abstract. Hollow steel-reinforced concrete-filled GFRP tubular member is a new kind of composite members. Firstly set the mold in the GFRP tube (non-bearing component), then set the longitudinal reinforcements with stirrups (steel reinforcement cage) between the GFRP tube and the mold, and filled the concrete between them. Through the axial compression test of the hollow steel-reinforced concrete-filled GFRP tubular member, the working mechanism and failure modes of composite members were obtained. Based on the experiment, when the load reached the ranges of 55-70% P_u (P_u -ultimate load), white cracks appeared on the surface of the GFRP tubes of specimens. At that time, the confinement effects of the GFRP tubes on core concrete were obvious. Keep loading, the ranges of white cracks were expanding, and the confinement effects increased proportionally. In addition, the damages of specimens, which were accompanied with great noise, were marked by fiber breaking and resin cracking on the surface of GFRP tubes, also accompanied with concrete crushing. The bearing capacity of the axially compressed components increased with the increase of reinforcement ratio, and decreased with the increase of hollow ratio. When the reinforcement ratio was increased from 0 to 4.30%, the bearing capacity was increased by about 23%. When the diameter of hollow part was decreased from 55mm to 0, the bearing capacity was increased by about 32%.

Keywords: GFRP tube; hollow steel-reinforced concrete-filled member; axial compression; mechanical property; experimental study

1. Introduction

Glass Fiber Reinforced Polymer (GFRP) was widely used in the field of civil engineering for its advantages of easy molding, high strength, high efficiency and corrosion resistance. FRP material has partially replaced steel in high-rise buildings, bridge pier, pile foundation and other civil engineering projects (Chen and Wang 2015, Abdelkarim and ElGawady 2016, Yang *et al.* 2017, Hadigheh *et al.* 2017, Setvati and Mustafa 2018). Hollow steel-reinforced concrete-filled GFRP tubular member is a new kind of composite member. Firstly set the mold in GFRP tube (non-bearing component), then set the longitudinal reinforcements with stirrups (steel reinforcement cage) between GFRP tube and the mold, and filled concrete between them. Not only does it achieve obvious economical effect on the construction cost, but also the column cross-sectional size is reduced. What's more, the use area of the building is increased, and the aesthetic requirement of the building is satisfied. In addition, the use of the hollow steel-reinforced concrete-filled GFRP tubular members in long-span bridges has greater potential. That is because the self-weight of long-span bridges often accounts for more than 60% of the total load. And if using the hollow

GFRP composite members, we can improve the rigidity of the bridge structure and increase the clearance under the bridge by reducing self-weight and cross-section height. More importantly, we can increase the service life of the bridge and reduce maintenance costs. Especially in foundation project with complex geological conditions including high salinity, high humidity and corrosion factors, the hollow steel-reinforced concrete-filled GFRP tubular members can overcome the corrosion effect. Therefore, hollow steel-reinforced concrete-filled GFRP tubular members have a broad application prospect in many important structures.

For GFRP member, the ideal force state is under axial compression. In recent years, many experts and scholars from all over the world have done some researches on compressed concrete-filled FRP tubular members, and have obtained series of research results. Nanni and Bradford (1995) conducted tests on concrete-filled FRP tubular columns under uniaxial compression. The results showed that the carrying capacity and ductility of concrete-filled FRP tubular columns were significantly higher than those of ordinary concrete columns. Mirmiran and Shahawy (1997) carried out axial compressive tests on concrete-filled FRP tubular columns, and concluded that the stress-strain curve of these members was double-line. Concrete-filled fiber-reinforced polymer tubes for axial and flexural structural members were made by Fam (2000). Huang *et al.* (2002) carried experiments on concrete-filled GFRP tubular columns under the axial compression. According to the test results, a model for the stress-strain relationship of the

*Corresponding author, Professor,
E-mail: chenbailing@mail.neu.edu.cn

^a Associate Professor, E-mail: bailingc@163.com

concrete-filled GFRP tubular column under the axial compression was set up, and the influence of the poisson ratio and load-sustain stress of the GFRP tubes on the strength of composite member was proposed. Yu *et al.* (2003) obtained the computational method of the deformation of concrete-filled FRP tubular short column under long-term load, and also analyzed the effects of some factors (FRP rate, axial compression ratio, loading age and holding time) on the deformation. Lu (2005) established the model of the relationship between stress and strain of FRP tube by analyzing the behavior of concrete-filled FRP tubular members under the axial compression, and compared the model with the experimental results. Teng *et al.* (2006) carried out the axial compression and four-point bending tests of FRP-concrete-steel tubular columns, and the experimental results showed that the FRP tube and the steel tube can effectively confine the internal concrete. Liu *et al.* (2007) carried out tests on GFRP-concrete circular tube columns under the axial compression. The failure modes of long columns and the relationship curves of load and strain were analyzed, and finally the computational formula of the carrying capacity was obtained. Wong *et al.* (2008) carried out a test of circular hollow FRP-confined concrete short columns under the axial compression. Doran *et al.* (2009) conducted a nonlinear analysis of rectangular and circular concrete-filled FRP tubular columns under the axial compression. Aire *et al.* (2010) performed experimental studies on concrete-filled FRP tubular columns. And based on the test results, the stress and the strain models of concrete-filled FRP tubular member were predicted. Realfonso and Napoli (2013) summarized the analytical models of compressive strength and ultimate strain of concrete-filled FRP tubular member, and also studied the ultimate strain of it. Yu and Teng (2013) carried out experimental research on FRP concrete-steel double-skin tubular columns with a square outer tube and a circular inner tube subjected to axial compression, and compared the experimental results with the theoretical analysis model. Zhang and Wang (2014) used finite element analysis software and non-linear analysis program to analyze the behavior of concrete-filled GFRP tubular members, steel-reinforced concrete-filled GFRP tubular members and GFRP-concrete-steel tubular members respectively under the axial compression, the eccentricity compression and the bending. Abdelkarim and ElGawady (2015) performed experimental studies on the behavior of concrete-filled fiber tubes (CFFT) polymers under axial compressive loading. Cascardi *et al.* (2016) summarized the existing analysis model of concrete-filled FRP tubular member, and

proposed the axially compressed hollow FRP-confined concrete models for circular and square sections. Wang *et al.* (2016) carried out series of tests, respectively on concrete-filled GFRP tubular members under the axial compression, and GFRP reinforced concrete members (under the axial, the eccentric compression and the bending). The effects on behavior of some main factors (including concrete strength grade, eccentricity, thickness of GFRP tube and reinforcement ratio) were analyzed, the non-linear analysis program was developed, and the computational formulas of composite members under the axial compression, the eccentric compression and the bending were obtained. Chellapandian *et al.* (2017) explores an innovative hybrid strengthening technique where short RC square column elements were strengthened using both Near Surface Mounted (NSM) CFRP laminates and Externally Bonded (EB) CFRP fabrics for confinement. Eid and Paultre (2017) analyzed compressive behavior of FRP-confined reinforced concrete columns.

In summary, at present many experts and scholars have done some researches related to compressed concrete-filled FRP tubular members, focusing on the stress-strain relationship and the compressive mechanical behavior of concrete-filled FRP tubular members and hollow concrete-filled FRP tubular members. However, there were few studies on the mechanical behavior of hollow steel-reinforced concrete-filled FRP tubular members under compression. Therefore, it is very necessary to study the mechanical performances of this kind of members.

2. Experimental program

2.1 Materials and parameters

A total of seven specimens were tested in the experimental program, including five hollow steel-reinforced concrete-filled GFRP tubular members (GRCH1, GRCH2, GRCH3, GRCH5 and GRCH6), one steel-reinforced concrete-filled GFRP tubular member (GRC4), and one hollow Concrete-filled GFRP tubular member (GCH7). And GFRP tubes were made by Shenyang Tianyang Glass Fiber Reinforced Polymer Co. Ltd. The fiber winding angle of all GFRP tubes was 80°. The diameters of all longitudinal steel bars and stirrups were respectively 14 mm and 8 mm. And stirrup spacing was 150 mm. Besides, the inner diameter and the wall thickness of the GFRP tubes were 200 mm and 5 mm respectively, and the length of the specimens was 700 mm. Fig. 1 shows the cross-sections of the specimens. The main experimental

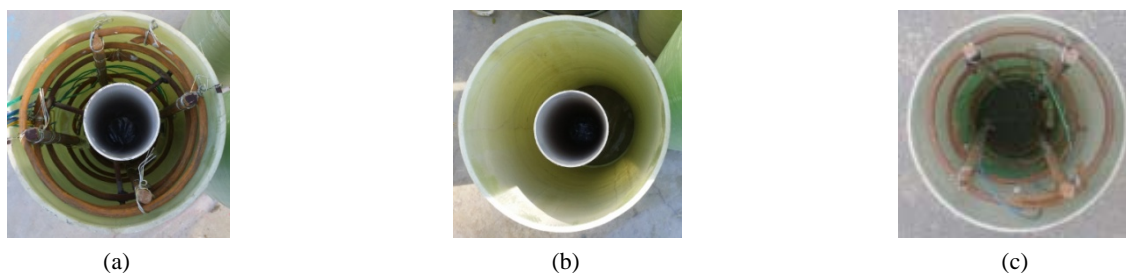


Fig. 1 Cross-section of test members

parameters used in the experimental program are given in Table 1. And the material properties are shown in Tables 2-3.

2.2 Fabrication of specimens

Before the experiment, GFRP tubes, PVC pipes (as a mold, non-bearing component), longitudinal steel bars and stirrups were prepared according to the design size. First, longitudinal steel bars and stirrups were bound to form the reinforced skeleton frame (steel reinforcement cage). Then the PVC pipe was fixed in the middle of the steel reinforcement cage with 3 equal-length steel bars (welded on the stirrups). After that, put the steel reinforcement cage

and PVC pipe into the GFRP tube, and ensure the PVC pipe was centered. Finally, poured concrete between GFRP tube and PVC pipe (GRC4 was poured in total section), and vibrated concrete fully. Making concrete cube blocks (150 × 150 × 150 mm) while pouring concrete. The compressive strength of the concrete cube blocks was 56.2 MPa. Fig. 2 shows the whole process.

2.3 Test contents and methods

(1) Test contents

The main contents of this experiment include:

- 1) Obtain the axial loads applied on specimens;
- 2) Measure the hoop and axial strains of GFRP tubes;
- 3) Measure the axial strains of longitudinal reinforcements and the hoop strains of stirrups;
- 4) Observe the axial deflection of specimens.

(2) Test methods

1) Measure strains

The longitudinal and lateral strain gages were attached to the four quadrant points of the middle sections of GFRP tubes to measure the axial and hoop strains of GFRP tubes; also attached strain gages to the middle of longitudinal steel bars and stirrups to measure the strains of longitudinal reinforcements and stirrups. Layout of strain gauges can be seen in Fig. 3(a).

2) Measure deflection

Large-range LVDT electrical displacement meters were arranged axially along test components in order to measure the axial deflection. Arrangement schematic of the displacement meters can be seen in Fig. 3.

2.4 Loading scheme

The GFRP tube and the core concrete were under compression jointly, and specimens were loaded directly via the upper and lower load-bearing plates. In order to prevent the local damage at the end of test components, special annular steel plate fixtures were fixed to the end of test components before loading. All specimens were loaded by monotonous multi-stage loading and using testing machine with a 5,000-kN capacity. The procedure was:

Table 1 Chart of experimental parameters and results

Specimen	Diameter of hollow part /mm	Number of steel bars	Ultimate bearing capacity /kN
GRCH1	75	4	2789
GRCH2	50	4	2940
GRCH3	110	4	2451
GRC4	-	4	3246
GRCH5	75	6	2889
GRCH6	75	8	3095
GCH7	75	-	2516

Table 2 Material properties of GFRP tubes

Circumferential		Longitudinal	
Elastic modulus /MPa	Strength /MPa	Elastic modulus /MPa	Strength /MPa
27210	467	16680	175

Table 3 Material properties of steel bar

Type of steel bar	Model	Yield strength /MPa	Ultimate tensile strength /MPa	Elongation /%
HPB235	φ8	271.1	361.2	20.9
HRB335	φ14	379.8	494.6	18.6



(a) Steel reinforcement cages



(b) PVC pipes

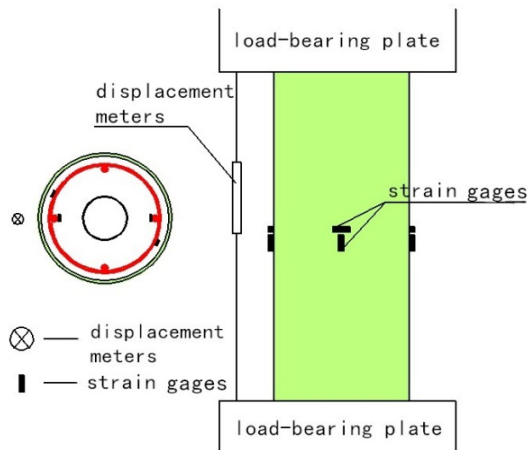


(c) Assembled component



(d) Finished test components

Fig. 2 Test component production



(a) Displacement meter and the strain gages layout



(b) Test device

Fig. 3 Schematic diagram of test device

- (1) The specimen was placed on both supports of tested and geometrically in the middle;
- (2) Preload and check if the test instruments worked properly, then unload to zero;
- (3) Monotonous multi-stage loading: The loading rate was 0.5 kN/s at the early stage of loading; when the load reached about 70% of the expected ultimate load of the specimen, the loading speed slowed down and the loading rate was changed to 0.2 kN/s; close to the failure, load continuously and slowly until the specimen damaged.

- (4) During loading, collect and record the instrument readings of each measure point, observe the deflection of specimens and the change of GFRP tube fiber.

Fig. 3(b) shows the test device.

3. Experimental phenomena and failure mode

At the early stages of loading, the deflections of specimens were very small and specimens were in the elastic stage. As the load approached about 55-70% P_u (P_u -ultimate load) (GRCH1: 52% P_u ; GRCH2: 58% P_u ; GRCH3: 60% P_u ; GRC4: 56% P_u ; GRCH5: 69% P_u ; GRCH6: 66% P_u ; GCH7: 55% P_u), the white cracks began to appear at the joint of specimens. With the increase of load, the color of the GFRP tube fiber changed from uniform light green to irregular local white. Keep loading, the range of the white cracks of the GFRP tube was expanding. When the load approached about the ultimate load, the fiber began to have frequent noise of fiber breaking and resin cracking. Until the load reached the ultimate load (GRCH1: 2789 kN; GRCH2: 2940 kN; GRCH3: 2451 kN; GRC4: 3246 kN; GRCH5: 2889 kN; GRCH6: 3095 kN; GCH7: 2516 kN), the fiber was broken at a certain distance from the top with great noise (GRCH1: 390 mm; GRCH2: 240 mm; GRCH3: 200 mm; GRC4: 350 mm; GRCH5: 260 mm; GRCH6: 300 mm; GCH7: 250 mm), which was stripped along the two sides from the fracture, and finally specimens were damaged. Fig. 4 shows the failure modes of specimens.

4. Load-strain behavior

Fig. 5 shows the curves of the longitudinal and hoop strains. (In these charts, the ordinate is the axial load, the positive abscissa is the circumferential strain of GFRP tubes (or stirrups), and the negative abscissa is the longitudinal strain of GFRP tubes (or longitudinal reinforcements)). From the result, we can find that with the increase of load, the strains of GFRP tubes, longitudinal reinforcements and stirrups show three stages: the initial straight-line stage, the elastic-plastic bending stage and the strengthened straight-line stage.

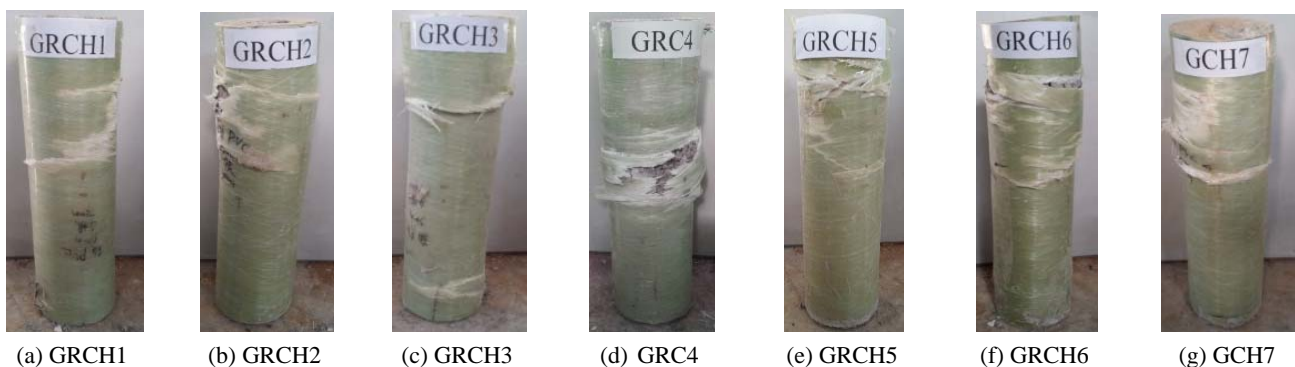


Fig. 4 Failure modes of specimens

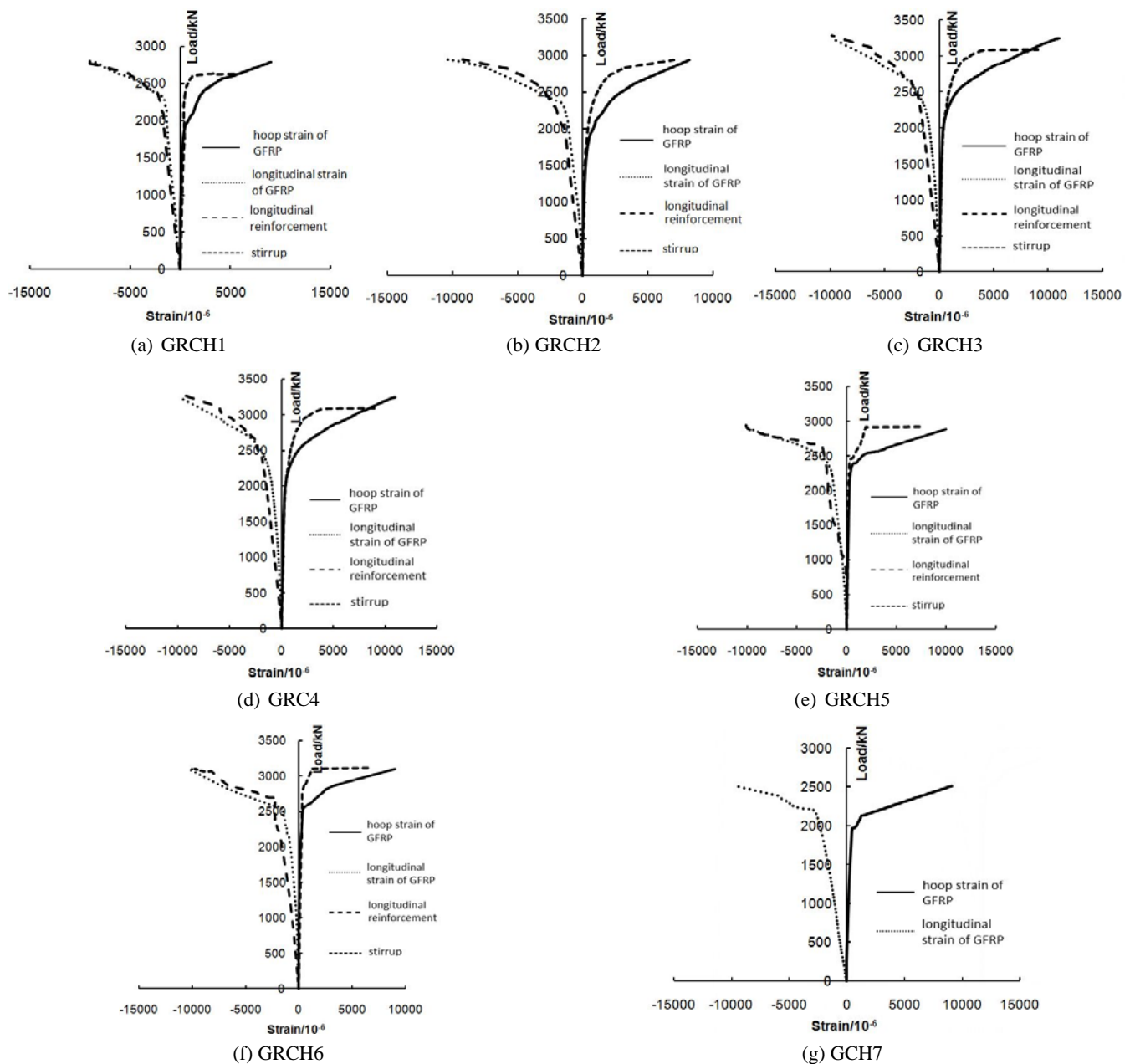


Fig. 5 Relationship curves of load and strain

(1) The hoop strain of GFRP tube

At the early stage of loading, the relationship between the hoop strain and the load was near linear, the specimen was in elastic stage, and the transverse deflection of concrete was small. During this stage, GFRP tube and concrete carried load independently, and their interaction was unobvious. When the load reached a certain value (GRCH1: $64\%P_u$, GRCH2: $59\%P_u$, GRCH3: $65\%P_u$, GRC4: $59\%P_u$, GRCH5: $69\%P_u$, GRCH6: $67\%P_u$, GCH7: $74\%P_u$), the increasing speed of the hoop strain of GFRP tube became faster than that of load. Furthermore, the increase of the transverse deflection of concrete led to the radial pressure between the concrete and the GFRP tube. And during this stage, the confinement effect of GFRP tube on concrete began to produce. As the load approached the ultimate load (GRCH1: $90\%P_u$, GRCH2: $85\%P_u$, GRCH3:

$86\%P_u$, GRC4: $88\%P_u$, GRCH5: $89\%P_u$, GRCH6: $93\%P_u$, GCH7: $93\%P_u$), the relationship between the load and the hoop strain of GFRP tube was near linear again, and the confinement effect got further strengthened. Until the load increased to the ultimate load, the hoop strain of GFRP tube reached limit value (GRCH1: 9012×10^{-6} , GRCH2: 8204×10^{-6} , GRCH3: 8999×10^{-6} , GRC4: 10905×10^{-6} , GRCH5: 9988×10^{-6} , GRCH6: 8990×10^{-6} , GCH7: 9097×10^{-6}).

(2) The longitudinal strain of GFRP tube

At the early stage of loading, the relationship between the increasing load and the increasing longitudinal strain was near linear. When the load reached a certain value (GRCH1: $68\%P_u$, GRCH2: $68\%P_u$, GRCH3: $60\%P_u$, GRC4: $60\%P_u$, GRCH5: $70\%P_u$, GRCH6: $70\%P_u$, GCH7: $72\%P_u$), the increasing speed of the longitudinal strain of

GRFP tube became faster than that of load, which meant the confinement effect GFRP tube on concrete had changed. As the load approached the ultimate load (GRCH1: $87\%P_u$, GRCH2: $89\%P_u$, GRCH3: $82\%P_u$, GRC4: $88\%P_u$, GRCH5: $89\%P_u$, GRCH6: $87\%P_u$, GCH7: $88\%P_u$), the relationship between the load and the longitudinal strain was near liner again, which meant the confinement effect was increased proportionally. Until the load increased to the ultimate load, the longitudinal strain of GFRP tube reached limit value (GRCH1: -9557×10^{-6} , GRCH2: -10368×10^{-6} , GRCH3: -9793×10^{-6} , GRC4: -9826×10^{-6} , GRCH5: -9597×10^{-6} , GRCH6: -10296×10^{-6} , GCH7: -9634×10^{-6}).

(3) The strain of longitudinal reinforcement

At the early stage of loading, the relationship between the increasing load and the increasing strain was near liner. When the load reached a certain value (GRCH1: $71\%P_u$, GRCH2: $69\%P_u$, GRCH3: $68\%P_u$, GRC4: $69\%P_u$, GRCH5: $75\%P_u$, GRCH6: $76\%P_u$), the increasing speed of the strain became faster than that of load. Until the load increased to the ultimate load (GRCH1: 2789 kN, GRCH2: 2940 kN, GRCH3: 2451 kN, GRC4: 3246 kN, GRCH5: 2889 kN, GRCH6: 3095 kN), the longitudinal reinforcement yielded and the strain reached limit value (GRCH1: -9557×10^{-6} , GRCH2: -9264×10^{-6} , GRCH3: -9350×10^{-6} , GRC4: -9858×10^{-6} , GRCH5: -10117×10^{-6} , GRCH6: -9799×10^{-6}).

(4) The strain of stirrup

At the early stage of loading, the relationship between the increasing load and the increasing strain was near liner. When the load reached a certain value (GRCH1: $80\%P_u$, GRCH2: $66\%P_u$, GRCH3: $75\%P_u$, GRC4: $66\%P_u$, GRCH5: $79\%P_u$, GRCH6: $80\%P_u$), the hoop strain of stirrup increased fast. As the load approached the ultimate load (GRCH1: $93\%P_u$, GRCH2: $89\%P_u$, GRCH3: $90\%P_u$, GRC4: $86\%P_u$, GRCH5: $94\%P_u$, GRCH6: $94\%P_u$), the stirrup began to yield. Until the load increased to the ultimate load, the strain of stirrup reached limit value (GRCH1: 5891×10^{-6} , GRCH2: 6991×10^{-6} , GRCH3: 7751×10^{-6} , GRC4: 9013×10^{-6} , GRCH5: 7692×10^{-6} , GRCH6: 6560×10^{-6}).

The above analysis shows that the change of strains is divided into three stages: the initial straight-line stage,

the elastic-plastic stage and the strengthened straight-line stage. It can also be concluded that the confinement effect of the GFRP tube on the core concrete was relatively obvious when the load reached about $70\%P_u$.

5. Effect of design parameters

(1) Effect of reinforcement ratio

The relationship curves between the load and the strains of test components with different reinforcement ratio were showed in Fig. 6. The reinforcement ratio of GRCH1 (including 4 longitudinal reinforcements) was 2.04%, that of GRCH5 (including 6 longitudinal reinforcements) was 3.06%, that of GRCH6 (including 8 longitudinal reinforcements) was 4.08%, and that of GCH7 (no longitudinal reinforcement) was 0.

The hoop strain of GFRP tube: at the early stage of loading, the reinforcement ratio had no effect on the strain. When the load reached about 1760 kN the effect was obvious, which meant the reinforcement ratio influenced the confinement effect of GFRP tube on concrete. Under the same load, for the test component with higher reinforcement ratio, the hoop strain of GFRP tube was smaller. Besides, at the same strain, the test component with higher reinforcement ratio could carry heavier load. However, the ultimate hoop strain of GFRP tube was similar.

The longitudinal strain of GFRP tube: at the early stage of loading, the reinforcement ratio had no effect on the strain. When the load reached about 627 kN, the effect was obvious. The curve slope of the test component with higher reinforcement ratio was relatively bigger, which meant the reinforcement ratio had effect on stiffness. Under the same load, the test component with higher reinforcement ratio had smaller longitudinal strain of GFRP tube. Besides, at the same strain, the test component with higher reinforcement ratio could carry heavier load. However, the ultimate longitudinal strain of GFRP tube was similar.

The strain of longitudinal reinforcement: The change regulation of the strain of longitudinal reinforcement was similar to that of GFRP tube. However, the yield load of longitudinal reinforcement was relevant to reinforcement ratio, and the ultimate strain of longitudinal reinforcement was similar.

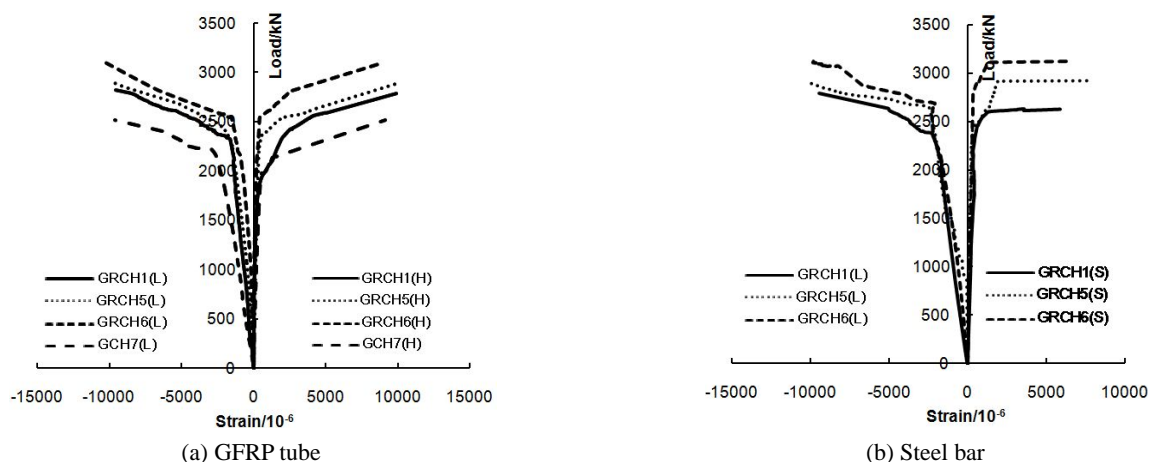


Fig. 6 Effect of reinforcement ratio

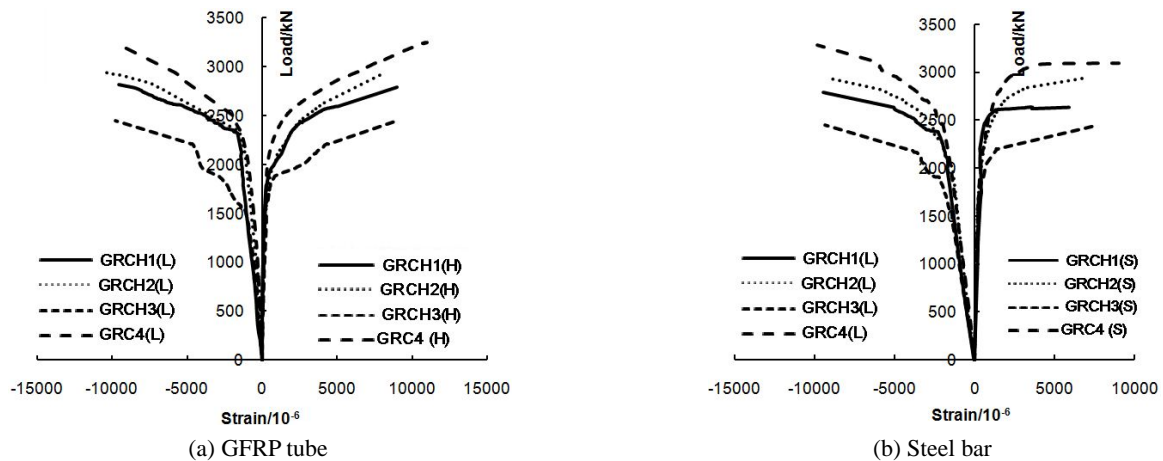


Fig. 7 Effect of hollow ratio

The strain of stirrup: The change regulation of the strain of stirrup was similar to that of GFRP tube. However, the yield load of stirrup was relevant to reinforcement ratio, and the ultimate strain of stirrup was similar.

Above all, when the load reached the range of 65-75% P_u , GFRP tubes had confinement effects on the core concrete. And the bearing capacity of the test components increased with the increase of reinforcement ratio. The range of yield load of longitudinal reinforcement was about 70-75% P_u , and that of stirrup was about 90% P_u . The hoop and longitudinal strains of all GFRP tubes almost reached the ultimate strain.

(2) Effect of hollow ratio

The relationship curves between the load and the strains of test components with different hollow ratio were showed in Fig. 7. The hollow ratio of GRCH1 (hollow part diameter 75 mm) was 12.8%, that of GRCH2 (hollow part diameter 50 mm) was 5.7%, that of GRCH3 (hollow part diameter 110 mm) was 27.4%, and that of GRC4 (hollow part diameter 0 mm) was 0.

The hoop strain of GFRP tube: at the early stage of loading, the hoop ratio had no effect on the strain. When the load reached about 1508 kN the effect was obvious, which meant the hollow ratio influenced the confinement effect of GFRP tube on concrete. Under the same load, the test component with lower hollow ratio had smaller hoop strain of GFRP tube. Besides, at the same strain, the test component with lower hoop ratio could carry heavier load. However, the ultimate hoop strain of GFRP tube was similar.

The longitudinal strain of GFRP tube: at the early stage of loading, the reinforcement ratio had no effect on the strain. When the load reached about 531 kN, the effect was obvious. The curve slope of the test component with lower hoop ratio was relatively bigger, which meant the hollow ratio had effect on stiffness. Under the same load, the test component with lower hollow ratio had smaller longitudinal strain of GFRP tube. Besides, at the same strain, the test component with lower hoop ratio could carry heavier load. However, the ultimate longitudinal strain of GFRP tube was similar.

The strain of longitudinal reinforcement: The change regulation of the strain of longitudinal reinforcement was similar to that of GFRP tube. However, the yield load of longitudinal reinforcement was relevant to hollow ratio, and the ultimate strain of longitudinal reinforcement was similar.

The strain of the stirrup: The change regulation of the strain of stirrup was similar to that of GFRP tube. However, the yield load of stirrup was relevant to hollow ratio, and the ultimate strain of stirrup was similar.

Above all, when the load reached the range of 60-65% P_u , GFRP tubes had confinement effects on the core concrete. And the bearing capacity of the test component increased with the decrease of the hollow ratio. The range of yield load of longitudinal reinforcement was about 70% P_u , and that of stirrup was about 90% P_u . The hoop and longitudinal strains of all GFRP tubes almost reached the ultimate strains.

6. Conclusions

Based on the above research work, the following conclusions have been drawn:

- When the load reached the range of 55-70% P_u , white cracks appeared on the surface of the GFRP tubes of specimens, and the confinement effect of the GFRP tube on the core concrete was obvious.
- The range of white cracks continued to expand with the increase of load, and the confinement effect increased linearly.
- Effect of reinforcement ratio on confinement effects: when the load reached the range of 65-75% P_u , GFRP tubes had confinement effects on the core concrete.
- Effect of hollow ratio on confinement effects: when the load reached the range of 60-65% P_u , GFRP tubes had confinement effects on the core concrete.
- The bearing capacity of the axially compressed components increased with the increase of reinforcement ratio, and decreased with the increase of hollow ratio. When the reinforcement ratio was increased from 0 to 4.30%, the bearing capacity was

increased by about 23%. When the diameter of hollow part was decreased from 55 mm to 0, the bearing capacity was increased by about 32%.

Acknowledgments

The research described in this paper was financially supported by the China Scholarship Council (No. 201406085029), the Fundamental Research Funds for the Central Universities (N120401010), the Natural Science Foundation of Liaoning Province (No. 20170540303) and the Natural Science Foundation of Liaoning Province (No. 20170540304).

References

- Abdelkarim, O. and ElGawady, M. (2015), "Concrete-filled-large deformable FRP tubular columns under axial compressive loading", *Fibers*, **3**(4), 432-449.
<https://doi.org/10.3390/fib3040432>
- Abdelkarim, O.I. and ElGawady, M.A. (2016), "Behavior of hollow FRP-concrete-steel columns under static cyclic axial compressive loading", *Eng. Struct.*, **123**, 77-88.
<https://doi.org/10.1016/j.engstruct.2016.05.031>
- Aire, C., Gettu, R., Casas, J.R., Marques, S. and Marques, D. (2010), "Concrete laterally confined with fiber-reinforced polymers (FRP): experimental study and theoretical model", *Mater. Constr.*, **60**(297), 19-31.
<https://doi.org/10.3989/mc.2010.45608>
- Cascardi, A., Micelli, F. and Aiello, M.A. (2016), "Unified model for hollow columns externally confined by FRP", *Eng. Struct.*, **1**(111), 119-130.
<https://doi.org/10.1016/j.engstruct.2015.12.032>
- Chellapandian, M., Prakash, S.S. and Sharma, A. (2017), "Strength and ductility of innovative hybrid NSM reinforced and FRP confined short RC columns under axial compression", *Compos. Struct.*, **176**, 205-216.
<https://doi.org/10.1016/j.compstruct.2017.05.033>
- Chen, B.L. and Wang, L.G. (2015), "Experimental study on flexural behavior of splicing concrete-filled GFRP tubular composite members connected with steel bars", *Steel Compos. Struct., Int. J.*, **18**(5), 1129-1144.
<https://doi.org/10.12989/scs.2015.18.5.1129>
- Doran, B., Koksals, H.O. and Turgay, T. (2009), "Nonlinear finite element modeling of rectangular/square concrete columns confined with FRP", *Mater. Des.*, **30**(8), 3066-3075.
<https://doi.org/10.1016/j.matdes.2008.12.007>
- Eid, R. and Paultre, P. (2017), "Compressive behavior of FRP-confined reinforced concrete columns", *Eng. Struct.*, **132**, 518-530.
<https://doi.org/10.1016/j.engstruct.2016.11.052>
- Fam, A.Z. (2000), "Concrete-filled fiber-reinforced polymer tubes for axial and flexural structural members", A dissertation submitted to the faculty of graduate studies in partial fulfillment of the requirements for the Degree of Doctor of Philosophy, National Library of Canada.
- Hadigheh, S.A., Gravina, R.J. and Smith, S.T. (2017), "Effect of acid attack on FRP-to-concrete bonded interfaces", *Constr. Build. Mater.*, **152**, 285-303.
<https://doi.org/10.1016/j.conbuildmat.2017.06.140>
- Huang, L.N., Zhang, D.X. and Wang, R.G. (2002), "Research on the stress-strain relation of the GFRP-confined concrete column under the axial compression", *J. Wuhan Univ. Technol.*, **24**(7), 31-34.
- Liu, J., Liu, Q.Y. and An, L. (2007), "Experimentation of GFRP-concrete circular tube columns", *J. Changchun Inst. Technol. (Natural Science)*, **8**(1), 11-13.
- Lu, G.C. (2005), "Study on behavior of concrete-filled FRP tubes under axial compression", Ph.D. Dissertation; Tsinghua University, Beijing, China.
- Mirmiran, A. and Shahawy, M. (1997), "Behavior of concrete columns confined by fiber composites", *J. Struct. Eng.*, **123**(5), 583-590.
[https://doi.org/10.1061/\(ASCE\)0733-9445\(1997\)123:5\(583\)](https://doi.org/10.1061/(ASCE)0733-9445(1997)123:5(583))
- Nanni, A. and Bradford, N.M. (1995), "FRP jacketed concrete under uniaxial compression", *Constr. Build. Mater.*, **9**(2), 15-124.
[https://doi.org/10.1016/0950-0618\(95\)00004-Y](https://doi.org/10.1016/0950-0618(95)00004-Y)
- Realfonso, R. and Napoli, A. (2013), "Confining concrete members with FRP systems: predictive vs design models", *Compos. Struct.*, **104**(5), 304-319.
<https://doi.org/10.1016/j.compstruct.2013.04.031>
- Setvati, M.R. and Mustaffa, Z. (2018), "Rehabilitation of notched circular hollow sectional steel beam using CFRP patch", *Steel Compos. Struct., Int. J.*, **26**(2), 151-161.
<https://doi.org/10.12989/scs.2018.26.2.151>
- Teng, J.G., Yu, T., Wong, Y.L., Dong, S.L. and Yang, Y.F. (2006), "Behavior of hybrid FRP-concrete-steel tubular columns: experimental and theoretical studies", *Progress Steel Build. Struct.*, **10**(5), 443-452.
- Wang, L.G., Han, H.F. and Liu, P. (2016), "Behavior of reinforced concrete-filled GFRP tubes under eccentric compression loading", *Mater. Struct.*, **7**(9), 2819-2827.
<https://doi.org/10.1617/s11527-015-0688-1>
- Wong, Y.L., Yu, T., Teng, J.G. and Dong, S.L. (2008), "Behaviour of FRP confined concrete in annular section columns", *Composites (Part B)*, **39**, 451-466.
<https://doi.org/10.1016/j.compositesb.2007.04.001>
- Yang, Y., Xue, Y., Yu, Y., Liu, R. and Ke, S. (2017), "Study of the design and mechanical performance of a GFRP-concrete composite deck", *Steel Compos. Struct., Int. J.*, **24**(6), 679-688.
<https://doi.org/10.12989/scs.2017.24.6.679>
- Yu, T. and Teng, J.G. (2013), "Behavior of hybrid FRP-concrete-steel double-skin tubular columns with a square outer tube and a circular inner tube subjected to axial compression", *J. Compos. Constr.*, **17**(2), 271-279.
[https://doi.org/10.1061/\(ASCE\)CC.1943-5614.0000331](https://doi.org/10.1061/(ASCE)CC.1943-5614.0000331)
- Yu, Q., Han, L.H. and Zhang, Z. (2003), "Long-term effect in FRP-confined concrete stub columns under sustained loading", *China J. Highway Transport*, **16**(3), 58-63.
- Zhang, N. and Wang, L.G. (2014), "Nonlinear analysis of flexural members of GFRP-concrete-steel double-skin tubular", *Steel Constr.*, **29**(12), 8-12.

CC